# Analysis of the dispersion compensation of acousto-optic deflectors used for multiphoton imaging

**Shaoqun Zeng***
Huazhong University of Science and Technology
Key Laboratory of Biomedical Photonics
Ministry of Education
Wuhan National Laboratory for Optoelectronics
Wuhan 430074 China
and
Yale University
Department of Neurobiology
New Haven, Connecticut 06511

**Xiaohua Lv***
**Kun, Bi**
**Cheng, Zhan and**
**Derong, Li**
Huazhong University of Science and Technology
Key Laboratory of Biomedical Photonics
Ministry of Education
Wuhan National Laboratory for Optoelectronics
Wuhan 430074 China

**Wei R. Chen**
**Wenhui Xiong**
Yale University
Department of Neurobiology
New Haven, Connecticut 06511

**Steven L. Jacques**
Oregon Health & Science University
OGI School of Science and Engineering
Beaverton, Oregon 97006

**Qingming Luo**
Huazhong University of Science and Technology
Key Laboratory of Biomedical Photonics
Ministry of Education
Wuhan National Laboratory for Optoelectronics
Wuhan 430074 China

**Abstract.** The acousto-optic deflector (AOD) is highly preferred in laser scanning microscopy for its fast scanning ability and random-addressing capability. However, its application in two-photon microscopy is frustrated by the dispersion of the AOD, which results in beam distortion and pulse lengthening. We report the analysis of simultaneous compensation for the angular dispersion and temporal dispersion of the AOD by merely introducing a single dispersive element such as a prism or a grating. Besides serving as a scanner, the AOD is also a part of the compressor pair by integrating the dispersive nature of the AO interaction. This compensation principle is effective for both one-dimensional (1-D) AOD and two-dimensional (2-D) AOD scanning. Switching from a 1-D to a 2-D system requires proper optical alignment with the compensation element, but does not involve any new components. Analytical expressions are given to illustrate the working principle and to help with understanding the design of the system. Fluorescence images of beads and cells are shown to demonstrate the performance of two-photon microscopy when applying this compensated 2-D AOD as scanner.  [DOI: 10.1117/1.2714061]

Keywords: multiphoton microscopy; scanning microscopy; femtosecond laser application; acousto-optic deflector; dispersion compensation.

Paper 06073R received Mar. 22, 2006; revised manuscript received Nov. 17, 2006; accepted for publication Dec. 8, 2006; published online Mar. 9, 2007.

## 1 Introduction

In the past 10 yr, multiphoton microscopy has helped to improve basic understanding about how brain cells work *in vivo*, covering both neuronal structure and function.[1] However, recording fast activation and information transmission in neuronal networks requires the use of two-photon microscopy to provide a better SNR and a faster imaging rate. These improvements are constrained mainly by the mechanical scanner commonly used in multiphoton microscopy. Actually, the acousto-optic deflector (AOD) is highly preferred for laser scanning microscopy because of its fast scanning ability, high stability, precision, and repeatability as it does not involve mechanical movement.[2,3] Moreover, two-dimensional (2-D) AOD scanning also enables random access to each pixel in the image field.[3] Random scanning regions of interest can devote dwell time to pixels of interest and omit unnecessary pixels, so that the SNR can be improved and the frame-capture rate increased. However, the dispersive nature of acousto-optic interaction and AOD materials causes both spatial and temporal dispersion of the ultrashort pulse laser radiation, which results in pulse broadening and beam distortion, and ruins the SNR and image resolution.[4,5] This effect has severely limited the application of 2-D AOD in multiphoton imaging microscopy.

*These authors contributed equally to this paper.
Address all correspondence to Shaoqun Zeng, Huazhong University of Science and Technology, National Laboratory for Optoelectronics, Wuhan 430074, China; Tel: 0086-27-87792033; Fax: 0086-27-87792034; E-mail: sqzeng@mail.hust.edu.cn

1083-3668/2007/12(2)/024015/7/$25.00 © 2007 SPIE

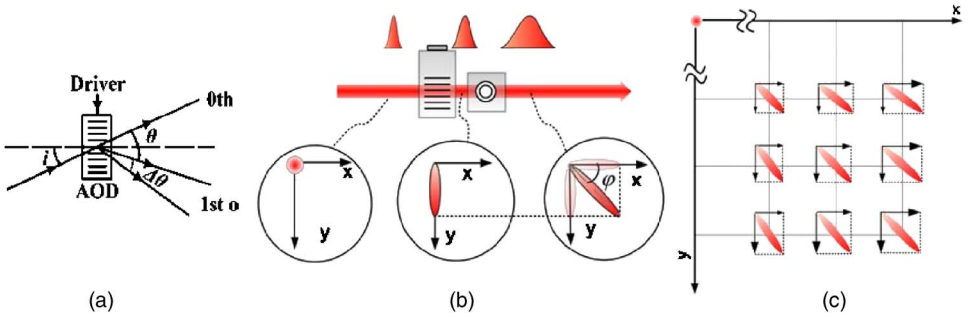


**Fig. 1** Ultrashort pulse laser radiation beam steered by AOD experiences spatial and temporal dispersion: (a) angular dispersion, (b) spot distortion and pulse broadening, and (c) scanning pattern.

Efforts have been undertaken to compensate for dispersion and apply the AOD as a scanner in two-photon microscopy.[5–8] By compensating for spatial dispersion and temporal dispersion separately with classic compensation schemes, Lechleiter et al.[6] and Roorda et al.[7] both applied 1-D AOD scanning to video-rate multiphoton microscopy. Iyer et al.[5] reported that with these classic pulse compressors and spatial dispersion compensation schemes the compensation system is quite complicated and is inefficient for 2-D AOD scanning. They recently proposed a noncompensating method using a laser with a longer pulse width and narrow spectral bandwidth to mitigate the dispersion problem to some extent.[8] This strategy decreases the peak power in individual laser pulses, and in turn reduces the SNR and spatial resolution. Actually, all these compensation methods have attempted to address spatial dispersion and temporal dispersion by using separate mechanisms and schemes.[5–7] However, the spatial dispersion and temporal dispersion of the grating are interconnected,[9] and thus the two kinds of dispersion of the AOD might be compensated for by one mechanism simultaneously. This would make the compensation scheme compact and more efficient. We previously reported on an experimental study of such a system, which used one single prism to compensate for both the spatial dispersion and the temporal dispersion of two orthogonal AODs simultaneously.[10] This paper extends this compensation prism to a general dispersive element, and gives a full account of the principle investigation, as well as experimental results with fluorescence imaging of biological samples. Specifically, the analytical expression is derived to describe the underlying mechanism of the simultaneous compensation and to help with the system design. As this is a basic technique for steering the femtosecond-pulse laser beam, it could be applied not only to two-photon microscopic imaging, but also to other fields such as second-harmonics imaging and micromachining, where fast steering of femtosecond-pulse laser radiation without dispersion is desired.

## 2 Principles and Methods

### 2.1 *Spatial and Temporal Dispersion*

As shown in Fig. 1(a), an active AOD works like a grating in which the deflection angle is wavelength dependent, given by[11]

$$\theta = \lambda f / \mathrm{V}, \tag{1}$$

where λ is wavelength of light in the vacuum, $f$ is the active frequency of the acoustic wave launched in the AOD crystal, and $V$ is the speed the acoustic wave travels in the crystal. As the ultrashort pulse laser radiation is nonmonochromatic, when deflected by an AOD, the output beam will be divergent as different spectra components exit at different deflection angles. As a result, the spectra components are spread along the direction in which the acoustic wave propagates, and form an elliptical spot.[12] This effect is known as spatial dispersion.[5–7] The angular dispersion of the active AOD $\sigma_A$ is responsible for the spatial dispersion, which can be derived by derivative Eq. (1) with regard to λ:

$$\sigma_A = \mathrm{d}\theta/\mathrm{d}\lambda = f/V. \tag{2}$$

Figure 1(b) shows a cartoon image of the spot shape changing due to spatial dispersion. The original round spot changes into an ellipse along the $Y$ axis after passing the $Y$ deflector, and twists an angle $\varphi$ [see the left insert in Fig. 1(b)] in relation to the $X$ axis after passing the second deflector ($X$ deflector); $\varphi = \arctan(f_y/f_x)$ and $f_x$ and $f_y$ are the active frequencies of the AOD $X$ and $Y$, respectively.[12] Thus, the integrated spatial dispersion for a 2-D AOD is the vector combination of the spatial dispersion of the two axes. Its orientation angle $\varphi$ is determined by the ratio of the active frequency of the two AODs. Figure 1(c) shows the scan pattern in part of the field of view (FOV). The orientation angle of each spot varies slightly across the FOV due to the different $X/Y$ frequency ratios of different positions.

Besides experiencing spatial dispersion, the ultrashort pulse laser radiation also experiences temporal dispersion, as different spectra components travel at different speeds in the acousto-optic crystal.[5–7] The pulse broadening effect is shown in Fig. 1(b).

### 2.2 *Basic Principle of Simultaneous Compensation for Spatial and Temporal Dispersion*

Examining the principle of the classic pulse compressor reveals the insight into the compensation principles proposed in this paper. The classic pulse compressor usually uses two dispersive devices to form a pair configuration.[13,14] The first dispersive device introduces angular dispersion, and a second dispersive device collimates the light beam. While a light

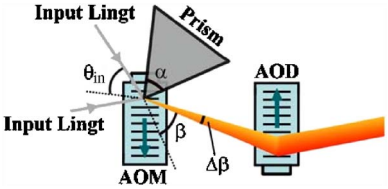


**Fig. 2** Pair configuration to simultaneous compensate both spatial and temporal dispersion of the AOD. The first element of the pair depicted here can be a prism or an AOM.

beam with angular dispersion propagates through the two dispersive elements, different components travel different optical paths, which introduces negative group delay dispersion (GDD). As a result, this system cancels the positive GDD in the optical path and compresses the pulse width. If the second dispersive element in the pair configuration is replaced with an AOD scanner, the principle of dispersion compensation still holds, as the AOD is also a dispersive element. In this way, both the spatial and temporal dispersion of the AOD is compensated for, while the original scanning function of the AOD is not disturbed. Figure 2 shows such an optical configuration, in which the prism or the AO modulator (AOM) is combined with the AOD to form a pair configuration to compensate for the dispersion of the AOD. From the view of the AOD scanner, only one single element (the first dispersive element in the pair configuration) is introduced to compensate for the spatial and temporal dispersion of the AOD. The AOD itself is a part of the compensation unit.

In general, any dispersive element that could provide angular dispersion could be used in the configuration shown in Fig. 2 to provide compensation. As shown later, a prism or an AOM would provide more flexibility in practical experiments. Here, an analytical expression for the prism and AOD is given to show the detailed compensation principle and the corresponding design rule. As 1-D analysis is more convenient to show the concept, the following derivation is first given for a 1-D AOD, and is then extended to a 2-D AOD. Based on these derivations, we discuss the features of each compensation configuration.

## 2.3 *Compensation with Prism*

### 2.3.1 *Spatial dispersion compensation*

Figure 3 shows the proposed compensation scheme with an isosceles-triangle prism, in which the angle transformation is labeled in the left insert. As shown in Fig. 3(b), a nonmonochromatic laser beam is incident at the prism at angle $\theta_{in}$ and exits the prism at angle $\beta$, although different spectral components exit the prism at different angles due to material dispersion $dn/d\lambda$. The angle transformation relation involved is given as

$$\sin\theta_{in} = n\sin\theta_1, \tag{3}$$

$$\sin\beta = n\sin\theta_2, \tag{4}$$

$$\theta_1 + \theta_2 = \alpha, \tag{5}$$

where $\alpha$ is the apex angle, and $n$ is the refractive index of the prism. Deriving Eqs. (3) to (5) with respect to $n$, and substituting Eqs. (3) and (5) into Eq. (4) we find

$$\frac{d\beta}{dn} = \frac{n\sin\alpha}{[1-n^2\sin^2\alpha-\sin^2\theta_{in}\cos 2\alpha+\sin 2\alpha\sin\theta_{in}(n^2-\sin\theta_{in})^{1/2}]^{1/2}(n^2-\sin^2\theta_{in})^{1/2}}. \tag{6}$$

The spatial dispersion constant is given by the angular dispersion[15]

$$\sigma_p = \frac{d\beta}{d\lambda} = \frac{d\beta}{dn}\frac{dn}{d\lambda}, \tag{7}$$

where $d\beta/dn$ is given in Eq. (6). Thus, from Eqs. (6) and (7), we see that the spatial dispersion constant $\sigma_p$ of the prism is dependent on the angle of incidence $\theta_{in}$, and the prism properties are material refractive index $n$, dispersion characteristics of the prism material $dn/d\lambda$, and apex angle $\alpha$.

The spatial dispersion constant as a function of angle of incidence is shown in Fig. 4 using an SF10 prism as an example. The material for SF10 prism is soft flint glass. The apex angle (45 deg, 60 deg, 65 deg) is labeled as the param-

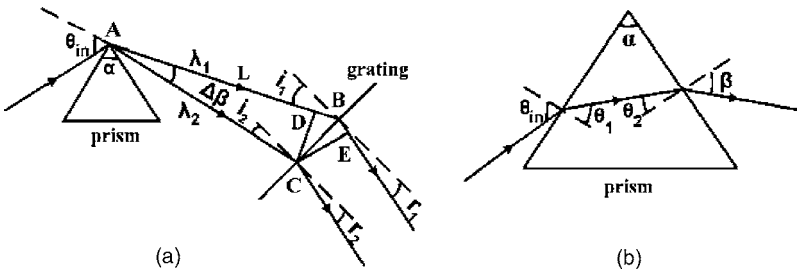


**Fig. 3** (a) Optical path of the prism-AOD configuration and (b) the angle transformation relation of the prism.

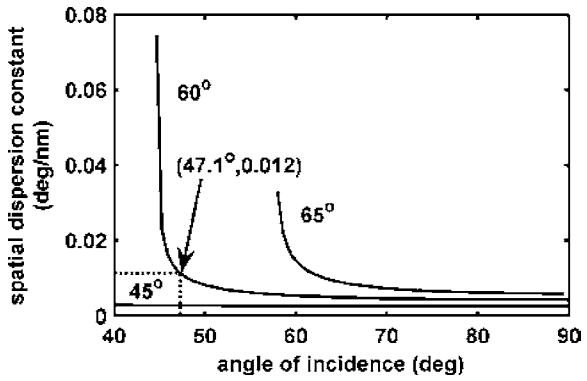


**Fig. 4** Spatial dispersion constant versus the angle of incidence at the prism, with the apex labeled for each curve. The arrow indicates the point enable spatial compensation for 2-D AOD.

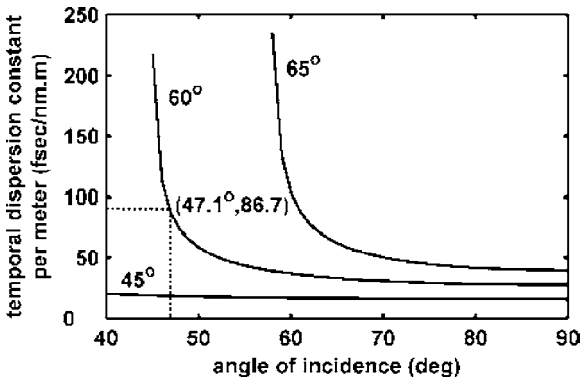


**Fig. 5** Temporal dispersion constant per meter versus the angle of incidence at the prism; the apex is labeled for each curve.

eter, and the wavelength is around 800 nm. It is shown that the dispersion constant increases inversely with the angle of incidence, and the critical point is different for different apex angles. Adjusting the angle of incidence of the prism would change the spatial dispersion constant. This actually provides flexibility in choosing prism to compensate for the spatial dispersion of a given AOD. It may be possible to select a moderate commercial prism and tune its angle of incidence to provide the required amount of angular dispersion compensation. The arrow in Fig. 3 shows the prism (SF10 prism; apex angle; 60 deg) with angle of incidence 47.1 deg, providing an angular dispersion constant of 0.012 deg/nm, which is ideal to compensate the integrated spatial dispersion of a 2-D AOD in our experiments.

In Fig. 4, curves with apex angles 45 and 65 deg give a rough measure of how large the spatial dispersion constant is for other potential prism candidates.

### 2.3.2 *Temporal dispersion compensation*

The temporal dispersion constant of the configuration shown in Fig. 3(a) can be derived by calculating the optical path difference between different spectra components. With similar treatment as in Ref. 16, the temporal dispersion constant can be written as

$$\frac{\Delta\tau}{\Delta\lambda} = -\frac{\lambda L}{c}\frac{\mathrm{d}\beta}{\mathrm{d}n}\frac{\mathrm{d}n}{\mathrm{d}\lambda}\frac{f}{\mathbf{V}}, \tag{8}$$

where $L$ is the distance between the prism and the AOD, and $\mathrm{d}\beta/\mathrm{d}n$ is as expressed in Eq. (6). Thus, the temporal dispersion constant of this configuration is dependent on $\theta_{\mathrm{in}}$, the prism properties $(\alpha, n, \mathrm{d}n/\mathrm{d}\lambda)$, and the AOD property $(f, V)$, and is proportional to $L$. The temporal dispersion constant per unit length for the prism-AOD configuration is shown as a function of the angle of incidence in Fig. 5, also with the apex angle as the parameter. Similar to the spatial dispersion constant, the temporal dispersion constant also increases inversely with the angle of incidence. The dashed line in Fig. 5 shows that in the case of spatial dispersion with a 2-D AOD (SF10 prism; apex angle, 60 deg; angle of incidence, 47.1 deg), the temporal dispersion constant of the prism is 86.7 fs/nm m.

The corresponding GDD is given as[9]

$$\mathrm{GDD} = \left(-\frac{\lambda^2}{2\pi c}\right)\frac{\Delta\tau}{\Delta\lambda}. \tag{9}$$

The material dispersion $\mathrm{d}n/\mathrm{d}\lambda$ is negative for most of the prism material (such as glass and $TeO_2$ crystal) in the spectral range from visible to near IR. Therefore, the GDD provided by this configuration is negative, and can compensate for the positive GDD introduced by the material dispersion of AOD crystal and other optical elements in the system, such as the objective. Figure 6 shows the GDD of this configuration as a function of the distance $L$, under these conditions: SF10 prism; apex angle, 60 deg; and angle of incidence, 47.1 deg. The GDD of a single AOD produced by the material dispersion is around 7000 $fs^2$. The star labeled in Fig. 6 shows that a distance of 35.5 cm is required to compensate for the GDD of a 2-D AOD.

These analytical expressions thoroughly explain the underlying mechanism of simultaneous compensation for the spatial and temporal dispersion of the AOD.

## 2.4 *Compensation with AOM*

When using the AOM as the dispersive element for compensation (see Fig. 2), the analytical expression is more straightforward, particularly when these two devices use the same material. As the AOM and AOD share the same angular dis-

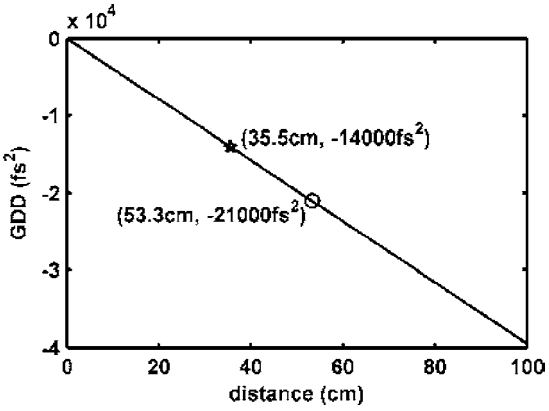


**Fig. 6** Negative GDD as a function of the distance, which is produced by angular dispersed beam traveling through the prism-AOD or AOM-AOD pair configuration.

persion expression, reversing the AOM with the acoustic wave traveling in a direction opposite to that of the AOD would provide the required spatial dispersion compensation. The temporal dispersion constant of the AOM-AOD configuration is given as[16]

$$\frac{\Delta\tau}{\Delta\lambda} = \frac{\lambda L}{c}\frac{f}{\mathbf{V}}\frac{f_{\mathrm{AOM}}}{\mathbf{V}}, \tag{10}$$

where $f_{\mathrm{AOM}}$ is the active frequency of the AOM.

Similar to the case of a prism-AOD configuration [see Eq. (8)], the temporal dispersion constant is also proportional to $L$. According to Eqs. (9) and (10), this configuration also provides negative GDD, which can also be tuned by adjusting $L$.

### 2.5 *Switch from 1-D Compensation to 2-D Compensation*

Switching from one AOD to two orthogonal AODs, the simultaneous compensation principle still holds, except moderate alignments are necessary. The differences of the 2-D AOD case over the 1-D AOD case are that the direction of the spatial dispersion of 2-D AOD is rotated 45 deg with regards to the 1-D AOD, and the amount of dispersion to be compensated for is larger. To balance these changes, rotation of the compensation elements is required to adjust the orientation of the spatial dispersion accordingly,[12] and then to decrease the angle of incidence at the prism (see Fig. 4) or increase the active frequency of the AOM [see Eq. (2)] to provide larger amounts of spatial dispersion compensation. After these alignments, the distance between the dispersive elements and the AOD was increased to negative GDD [see Eqs. (8) to (10)] and reached optimized temporal dispersion compensation for 2-D AOD.

## 3 Experimental Results and Discussion

### 3.1 *Two-Photon Imaging with 2-D AOD Compensated with a Prism*

The first trial of this principle is implemented by using a prism (SF10 prism; apex angle, 60 deg) as the compensation element. Preliminary results showed that with an angle of incidence of 47.1 deg and $L$=35.0 cm, the beam spot and pulse width exiting the 2-D AOD were recovered.[10] To further confirm the compensation results, 170-nm-diam microscophere fluorescence beads (P7220, Molecular Probes) and fluorescent epithelium cells were imaged with a custom-built two-photon microscope employing the compensated 2-D AOD as the 2-D scanner, as shown in Fig. 7.

Figure 7(a) is the image of the 170-nm beads. The corresponding spatial resolution is 0.305 $\mu$m. Figure 7(b) is the fluorescence image of an epithelium cell, where a filament as small as 300 nm can be clearly resolved.

### 3.2 *Two-Photon Imaging with 2-D AOD Compensated with an AOM*

In our experiments, a $TeO_2$ AOM similar to the AOD is applied in the AOM-AOD configuration, to compensate for the dispersion. A femtosecond-pulse laser radiation source (Model: Maitai BB, Spectra Physics) delivers laser pulses with pulse width of 120 fs, as measured with an autocorrelator (standard error, 5 fs). The active frequency of the AOM is set to be 96 MHz, with a beam expander (not shown in Fig. 8) to increase the angular dispersion 1.4× to provide optimal spatial dispersion compensation. It is observed as expected that collimated beam exits the 2-D AOD activated at the center frequency. This proves that the spatial dispersion is well compensated. For temporal dispersion compensation, the distance $L$ is tuned to be 70.0 cm to achieve optimized pulse width (128 fs) at the center frequency of the 2-D AOD. This value of $L$ is larger than the expected 53.3 cm for compensation of the GDD of the three AO devices (see the circle labeled in Fig. 6). The extra GDD is probably introduced by an intensity attenuator in the optical path.

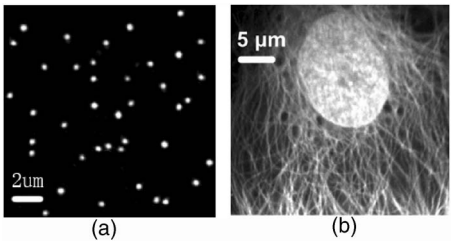


**Fig. 7** Fluorescence images obtained with a two-photon microscope with the prism as the compensation element of (a) 170-nm beads and (b) an epithelium cell.

To show the performance of dispersion compensation with AOM, the 2-D AOD compensated with an AOM is also applied as a 2-D scanner in a custom-built two-photon microscope. The schematic diagram was shown in Fig. 8. As shown there, the AOM is rotated (45 deg) with regard to the 2-D AOD. Between the AOM and the AOD, a half-wave plate (HWP) was placed to adjust the polarization to be optimized for the AOD.

Figure 9 shows fluorescence images obtained with this two-photon microscope with an AOM as the compensation element. Figure 9(a) is an image of 170-nm-diam fluorescent microsphere beads, which indicates the spatial resolution of this two-photon microscope is about 0.325 $\mu$m. Figure 9(b) shows the fluorescence image of an epithelium cell, where a filament as small as 300 nm can be clearly resolved. These

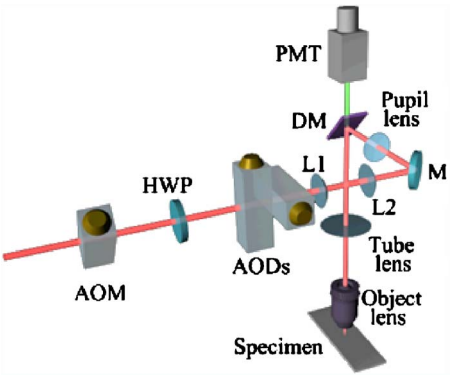


**Fig. 8** Schematic diagram of a custom-built two-photon microscope with an AOM-compensated 2-D AOD as the beam scanner. DM: dichroic mirror; PMT: photomultiplier tube; L1: lens 1; L2: lens 2; M: mirror.

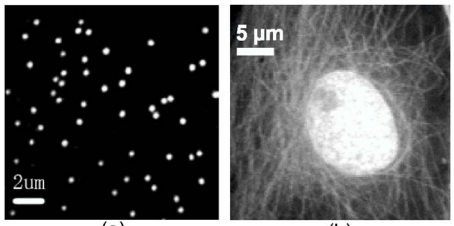


**Fig. 9** Fluorescence images obtained with a two-photon microscope with the AOM as the compensation element of (a) 170-nm beads and (b) an epithelium cell.

results show the overall performance of using this compensated 2-D AOD in two-photon microscopic imaging.

## 4 Discussion

In this paper, a single dispersive element was proposed to compensate for the spatial and temporal dispersion produced during AOD scanning ultra-short-pulse laser radiation. The mechanism was then revealed with analytical expression and verified with experiments.

Multiphoton microscopic imaging with an AOD scanning femtosecond-pulse laser radiation is important to biological studies.[4] In efforts to address the dispersion of AOD-based multiphoton microscopy, a prism is widely applied to perform spatial dispersion compensation.[5–7] Similarly, in an effort to steer ultra-short-pulse laser radiation for laser micromachining,[12] an AOM is proposed to serve the same function. The prism or AOM were not considered to compensate for the temporal dispersion. A separate and independent system was applied to provide temporal compensation.[5–7]

Contrary to the previously reported strategy of separate compensation of the spatial and temporal dispersion in AOD-based multiphoton microscopy,[5–7] this paper proposed the new strategy of simultaneous compensation by integrating the dispersive nature of the AO interaction. It then proposed a scheme to implement this strategy by introduction only one single dispersive element. The whole system is compact and with higher efficiency for the sake of simple optics configuration. This strategy and its implementation are particularly useful for 2-D AOD scanning multiphoton microscopy, as switching from 1-D AOD scanning to 2-D AOD scanning requires only proper alignments rather than additional optics. In addition, increasing the amount of temporal dispersion compensation is realized equally by adjusting the angle of incidence or active frequency rather than merely increasing the separation between the compensation element and the AOD. This feature, in turn, simplifies the optical configuration for 2-D AOD scanning. As a result, two-photon microscopic imaging using 2-D AOD with high efficiency was realized.

The concept of simultaneous compensation was demonstrated with both the prism and the AOM compensation schemes. Compensation with another dispersive element grating (not the AO type) is also possible, but is less flexible as the angular dispersion constant set by the grating period is fixed. For prism and AOM compensation schemes, from the fluorescence images presented here, obtained with the two-photon microscopes, no significant differences were observed. Actually each scheme has its own features. The configuration with the AOM is more convenient for optical alignment, and alignment error can be balanced by electrically adjusting the active frequency of the compensation AOM. On the other hand, the material-dispersion-induced GDD of the AOM configuration is about 50% higher than that of the prism case, as the number of the highly dispersive AO crystals in the optics path increases. This requires longer separation $L$, which is constrained by the optical window size of the AOD. Another issue involved in the prism configuration is the transmission rate. Tuning the angle of incidence at the prism to adjust angular dispersion and temporal dispersion would sometimes change the transmission rate of the prism due to the Fresnel losses.[12,17,18] This should be considered when the laser radiation power is precious. One possible solution is to use a specially designed prism for a given 2-D AOD rather than off-the shelf prisms. According to Eqs. (6) and (7), by selecting a higher dispersion material and designing the apex angle, it is possible to obtain angular dispersion compensation with incidence at the Brewster angle, and ensure maximum transmission. Another benefit for higher material dispersion $dn/d\lambda$ in the prism scheme is that the system would be more compact. According to Eqs. (8) and (9), the negative GDD provided is proportional to the product of the distance $L$ and material dispersion $dn/d\lambda$; a larger $dn/d\lambda$ results in a smaller $L$. A $TeO_2$ prism has larger material dispersion than the SF10 prism,[17] and the compensation scheme with a $TeO_2$ prism will be smaller in size.

One more concern in our experiments is the polarization optimization in the 2-D AOD scanning. Actually, this is dependent on the AOD working mode. As the AOD crystal used here is $TeO_2$, the AOD operates in the slow-shear mode under the abnormal Bragg condition. This kind of AOD operates on a signal polarization, and rotates the polarization of the exit beam 90 deg with regard to the input polarization.[16] Therefore, an HWP is inserted right after the compensation element to adjust the polarization and match that of the first AOD (see Fig. 8). The laser polarization exiting the first AOD inherently matches that of the second AOD. Other kinds of AODs not working in this mode do not require this HWP to optimize the polarization.

One limitation remains for this concept of compensation: the residual dispersion. As the dispersion of the active AOD is frequency dependent, it varies[12] across the FOV. In this method, the angular dispersion compensation provided is constant. Therefore, the temporal and spatial dispersion are exactly compensated only in the point of the FOV (the center in our experiments), the residual temporal and spatial dispersions in the other pixels of the FOV were improved about 80% relative to the uncompensated 2-D AOD. A problem would arise when the technique is applied to immunohistochemical analysis of the detailed fine structure of biological samples. While for functional studies, where the relative change in signal intensity due to stimulation is of higher concern, this would not be a problem. A more flexible method to provide real-time compensation to each pixel of the FOV is under investigation.

## 5 Conclusion

We proposed and demonstrated that a single dispersion element such as a prism or an AOM can simultaneously compen-

sate both the temporal and spatial dispersion induced by a 2-D AOD, and thus validates its application as a 2-D scanner for femtosecond-pulse laser radiation in multiphoton microscopy. Such a compact scheme will also have great potential in other fields where 2-D AODs are used to steer femtosecond-pulse laser radiation free of dispersion.

## Acknowledgments

The authors would like to express special thanks to L. Wang and L. Fu for helpful discussions. The work was supported by National Science Foundation of China (NSFC) Grants 30370463, 60278017, 30328014, the 973 Program: 2004CB520804, and National Institutes of Health (NIH) Grant 5R01DC003918 to W.R.C.

## References

1. K. Svoboda and W. Denk, "Photon upmanship: why multiphoton imaging is more than a gimmick," *Neuron* **18**, 351–357 (1997).
2. S. R. Goldstein, T. Hubin, S. Rosenthal, and C. Washburn, "A confocal video-rate laser-beam scanning reflected-light microscopy with no moving parts," *J. Microsc.* **157**, 29–38 (1990).
3. S. Bullen, S. Patel, and P. Saggau, "High-speed, random-access fluorescence microscopy: I. High-resolution optical recording with voltage-sensitive dyes and ion indicators," *Biophys. J.* **73**, 477–491 (1997).
4. W. Denk, D. W. Piston, and W. W. Webb, "Two-photon molecular excitation in laser-scanning microscopy," in *Handbook of Biological Confocal Microscopy*, J. B. Pawley Ed., pp. 445–458, Plenum, New York (1995).
5. V. Iyer, B. E. Losavio, and P. Saggau, "Compensation of spatial and temporal dispersion for acousto-optic multiphoton laser-scanning microscopy," *J. Biomed. Opt.* **8**, 460–471 (2003).
6. J. D. Lechleiter, D. T. Lin, and I. Sieneart, "Multi-photon laser scanning microscopy using an acoustic optical deflector," *Biophys. J.* **83**, 2292–2299 (2002).
7. R. D. Roorda, T. M. Hohl, R. Toledo-Crow, and G. Miesenbock, "Video-rate nonlinear microscopy of neuronal membrane dynamics with genetically encoded probes," *J. Neurophysiol.* **92**, 609–621 (2004).
8. V. Iyer, T. Hoogland, B. E. Losavio, R. Fink, R. Gaddi, S. Patel, A. Larson, and P. Saggau, "Acousto-optic multiphoton laser scanning microscopy (AO-MPLSM) for structural and functional imaging in living brain slices," in *Multiphoton Microscopy in the Biomedical Sciences V*, A. Periasamy and P. T. C. So, Eds., *SPIE* **5700**, 90–102 (2005); also *J. Neurophysiol.* **95**, 535–545 (2006).
9. J. C. Diels and W. Rudolph, *Ultrashort Laser Pulse Phenomena: Fundamentals, Techniques, and Applications on a Femtosecond Time Scale*, Academic Press, San Diego (1996).
10. S. Zeng, X. Lv, C. Zhan, W. R. Chen, W. Xiong, S. Jacques, and Q. Luo, "Simultaneous compensation of spatial and temporal dispersion of acousto-optical deflectors for two-dimensional scanning with a single prism," *Opt. Lett.* **31**, 1091–1093 (2006); http://ol.osa.org/abstract.cfm?id=88941.
11. R. W. Dixon, "Acoustic diffraction of light in anisotropic media," *IEEE J. Quantum Electron.* **QE-3**, 85–93 (1967).
12. B. K. A. Ngoi, K. Venkatakrishnan, B. Tan, P. Stanley, and L. E. N. Lin, "Angular dispersion compensation for acousto-optic devices used for pulsed-pulsed laser micromachining," *Opt. Express* **9**, 200–206 (2001); http://www.opticsexpress.org/abstract.cfm?URI=OPEX-3-9-332.
13. E. B. Treacy, "Optical pulse compression with diffraction gratings," *IEEE J. Quantum Electron.* **QE-5**, 454–458 (1969).
14. R. L. Fork, O. E. Martinez, and J. P. Gordon, "Negative dispersion using pairs of prisms," *Opt. Lett.* **9**, 150–152 (1984).
15. W. J. Smith, *Modern Optical Engineering*, Chap. 2, McGraw-Hill, NewYork (2000).
16. M. Nakazawa, T. Nakashima, and H. Kubota, "Optical pulse compression using a $TeO_2$ acousto-optical light deflector," *Opt. Lett.* **13**, 120–122 (1988).
17. M. Nakazawa, T. Nakashima, H. Kubota, and S. Seikai, "Efficient optical pulse compression using a pair of Brewster-angled $TeO_2$ crystal prisms," *J. Opt. Soc. Am. B* **5**, 215–221 (1988).
18. M. Born and E. Wolf, *Principles of Optics*, Chap. 1, Pergamon, London (1980).